2019 32nd International Conference on VLSI Design and 2019 18th International Conference on Embedded Systems (VLSID)

Structural and Behavioural Facets of Digital Microfluidic Biochips with Hexagonal-Electrode-based Array

Amartya Dutta[1], Riya Majumder[2], Debasis Dhal[3], and Rajat Kumar Pal[3]
[1]Department of Computer Science and Engineering, B. P. Poddar Institute of Management and Technology, Kolkata, India
[2]Department of Computer Science and Engineering, Supreme Knowledge Foundation Group of Institutions, West Bengal, India
[3]Department of Computer Science and Engineering, University of Calcutta, Kolkata, India
{dutta.kultu, riyamanai, debasisdhal06, pal.rajatk}@gmail.com

***Abstract*— In recent times, digital microfluidic biochips have received an appreciable recognition as one of the most promising platforms for lab-on-a-chip attainment. Such a compound system can replace most of the laboratory experiments by controlling nano-litre or micro-litre volume of droplets and yield more accurate and faster results depending upon electrowetting on dielectric (EWOD) principle. Being aware of the fact about the progress of traditional square electrode biochips in the digital microfluidic realm, here in this paper, we present two-dimensional regular hexagonal digital microfluidic electrode (HDMFB) array. A hexagonal chip array offers numerous advantages over a square array like droplet movement, mixing operation, speed, etc. To cope with this new design technique care should be taken for fluidic constraints and electrode constraints to ensure safe droplet routing. Here, we propose an algorithm for efficient control pin assignment on the chip such that no droplet interference on the chip array occurs during an assay operation. Moreover, a multiplexed assay operation is performed by a scheduling algorithm, and the result is compared with a previous work conducted on the conventional square electrode array. Finally, a comparative study is done on the proposed architecture and the existing one on some relevant issues.**

***Keywords*—** Lab-on-a-chip, Bioassay, DMFB, HDMFB, BSA-7 algorithm, PCB layer, Mixing operation, Routing.

I. Introduction

Nowadays microfluidic-based digital biochips are drawing much attention for biomedical and biochemical purposes. This encompasses biology with electronics and forms the composition of a bio-micro-electro-mechanical system [1], which is addressed as lab-on-a-chip [2], [3]. The digital microfluidic systems offer some advantages over the conventional laboratory procedures. Advancement in microfluidic technologies grows up its possibilities in several areas like different enzymatic analysis, DNA detection and analysis, proteomic analysis involving proteins and peptides, immunoassays, various toxicity monitoring, and several biomedical testing [2], [3].

In contrast to the first generation of microfluidic biochips [1], which were based on the principle of continuous fluid flow, a more promising alternative is referred to as digital microfluidics [4], [5]. This second-generation digital microfluidic system [1] manipulates liquids as discrete droplets in a digital manner and follows electrowetting on dielectric (EWOD) principle [3]. This emerging trend offers a novel approach that handles the droplets of nano-litre or micro-litre volume and provides high speed in droplet routing, energy efficiency, less error in testing, and scalable system architecture based on a two-dimensional (2D) microfluidic array of identical basic unit cells [4]. Though we are more familiar with the basic cells like square electrode, the new design techniques for digital microfluidic biochip (DMFB) with equilateral triangular electrode array [6], [7], and regular hexagonal shaped electrode array [3] are also feasible and applicable.

In this paper, we have discussed the geometrical shift in designing of DMFB from square electrode cell to hexagonal one and how the fundamental operations of microfluidics, like droplet transportation, mixing and other design issues which may lead to the betterment of bioassay operations [3], [4], [5]. We denote this regular hexagonal 2D electrode array as HDMFB. In this context, we have mentioned the design of hexagonal electrode, droplet routing constraints like fluidic and electrode constraints, and pin assignment algorithm to carry out the bioassay operations in the proposed model.

II. Preliminaries

In this section, we like to address the architectural representation of DMFB, its working principle, and the size of a droplet in terms of square electrodes briefly. Routing of the droplet on the DMFB chip is managed with the help of EWOD principle. Electrowetting on dielectric uses DC voltages to control the interfacial energy between the liquid (biological sample or reagent) and the solid substrate (electrode) so that liquid droplet can route through the electrode array. In the architectural scenario of DMFB, the droplets are sandwiched between two parallel plates, where the bottom and top plates are made up of (discrete) electrode array and continuous ground plate, respectively [4], [5]. The upper plate consists of a transparent continuous ground electrode of conductive indium-tin-oxide (ITO).

Because of DC voltage V that is applied between the electrode (solid) and the droplet (liquid), the charge is accumulated in the droplet as well as in the electrode, and the electrostatic energy is stored in the droplet. Thus, the solid-liquid interfacial tension between the solid and the liquid decreases that yields a change in the shape of the droplet [4]. More specifically the contact angle between the solid and liquid is reduced. When the voltage is applied to the adjacent electrodes, the droplet will tend to increase its contact area, and hence the droplet movement occurs on the chip. Thus, through simultaneous activation and deactivation of adjacent electrodes on the chip, droplet transportation, splitting, mixing can easily be controlled. An assay operation is a combination of all the operations like the creation of droplets, routing, mixing, and detection.

III. Problem under Consideration

Though square electrode microfluidic biochip is more commonly used and favoured layout in the microfluidic application domain, it has some limitations. In the square cell, the droplet may route in only four directions and follows the Manhattan distance, whereas, in the case of the equilateral triangular electrode, a droplet may move in three directions only. In addition to that, in the case of the triangular electrode, the vertical movement is restricted [7]. To overcome these inadequacies, we concentrate on the geometrical shape of the electrodes, and as a result, an architectural shift is made from a square shaped cell to a 2D regular hexagonal cell. The hexagonal array offers a closed

2380-6923/19/$31.00 ©2019 IEEE
DOI 10.1109/VLSID.2019.00060

packing design [8] where the six-sided shape fits together perfectly in the array.

DMFB with hexagonally shaped electrode array (HDMFB) is expected to increase the droplet transportation very effectively because a droplet motion can be governed in both horizontal and diagonal directions to six direct neighbours. Also, the mixing operation may lead to the betterment of the assay outcome as phase changes of droplet trace are only 0° and 60°, which are described later in this paper. It is supposed to get better mixing operation [10] in hexagonal biochip because the droplet motion may be controlled in the zigzag or linear form in six different directions as per the requirement during the assay operation.

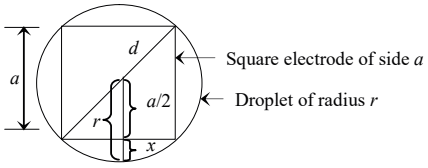

Fig. 1. Top view of a droplet placed on a charged square electrode.

In this framework, we have designed the hexagonal electrode cell, droplet routing restrictions like fluidic constraints and electrode constraints, and the most effective mixing operation. An efficient control pin assignment algorithm is also proposed to avoid unwanted droplet mixing and splitting. Finally, a complete bioassay operation is carried out and the total assay completion time is compared with respect to the square electrode array.

IV. Methodology

The amount of time in terms of steps required to complete an assay successfully is considered as a measurement of whether the new design technique is appreciable. Existing routing examples in square cells are tailored into HDMFB to determine the effectiveness of this new design. Now we demonstrate the droplet routing and modifications of fluidic constraint due to this geometrical replacement from square cells to HDMDB.

A. Calculation of the value of x

When the adjacent electrodes in the chip array are activated and deactivated simultaneously, with respect to the previous one, a droplet advances from an electrode to its adjacent one due to the change in surface tension. To sustain the voltage amount constant while shifting from the square cell to hexagonal one, we assume the overlapped portion of the droplet over its next adjacent cell, where the droplet may move, is fixed. Hence, keeping the side of the square electrode as a reference, we can get a relation between the sides of a hexagonal electrode with that of a square electrode. Fig. 1 shows the top view of a droplet of radius r on a charged square electrode. Here x denotes the portion of the droplet outside the electrode. Primarily, x is measured along the radius of the droplet on the charged electrode as shown in Fig. 1.

B. The side of the regular hexagonal electrode

Fig. 2 shows the top view of a droplet when it is put on an activated hexagonal shaped electrode. Fig. 3 is referred top view of a regular hexagonal array with saw teeth, where a droplet can move through six sides of a hexagon.

Here two assumptions are taken into consideration; the droplet volume on the hexagonal electrode is same as that on the square electrode, and the outer portion of a droplet remains unchanged as it is kept on a square cell. Let the radius of the droplet be r, and the side of the regular hexagon be y. As we know that a regular hexagon consists of six equilateral triangles, we can conclude that the side of the hexagon is equal to the radius of the droplet, i.e. $y = r$. Hence, $h^2 + (r/2)^2 = r^2 \Rightarrow h = \sqrt{3}/2 \times r$.

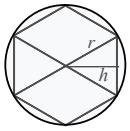

Fig. 2. Top view of a droplet placed on a charged hexagonal electrode.

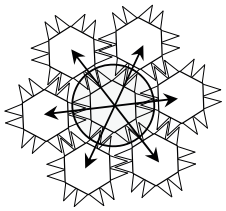

Fig. 3. Top view of a regular hexagonal array, where a droplet can move through all the six sides of a hexagon. The saw teeth cover the gap between two adjacent electrodes, and it overcomes leakage.

Applying the assumption that the spread of droplet is the same on the square and hexagonal electrode, we can write $h + 0.207a = r$. Also applying the first assumption, we can write $r = a/\sqrt{2}$. So, $h + 0.207a = a/\sqrt{2}$. Thus, $h = 0.5a$. We have already deduced the height of the equilateral triangle in a hexagon, $h = \sqrt{3}/2 \times r$. Now replacing the value of h, we get $0.5a = \sqrt{3}/2 \times r$. As $y = r$, we get $y = 0.58a$. This is the relationship between the side of the regular hexagonal shaped electrode and the square electrode. We can also derive the size of the hexagonal electrode with respect to a square cell, $A_{\text{hexagon}} = 3\sqrt{3}/2 \times y^2 = 2.598 \times (0.58a)^2 = 0.87a^2$.

Thus, the area of the hexagonal cell is smaller than the area of the square cell. In practical design, the top view of a hexagonal array looks as in Fig. 3, due to the presence of the saw teeth, and the figure also indicates all possible movements of a droplet in the electrode array.

C. On-chip pin planning

This section concentrates on the application of independent pin constraint chip design problem for 2D HDMFB. Our goal is to calculate the minimum number of control pins required for conducting any assay operation on the chip so that no droplet interference occurs.

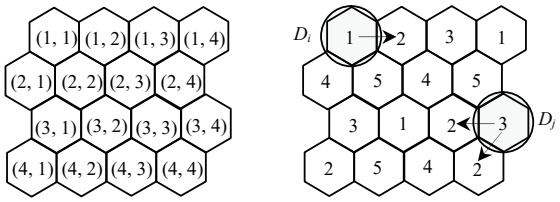

Fig. 4. (a) The coordinate mapping on the hexagonal chip array. (b) An arbitrary pin assignment in these coordinate locations and droplet interference.

The graphical description of a 4×4 hexagonal electrode array with five control pins is shown in Fig. 4. These pins are assigned arbitrarily. Suppose, droplet D_i is placed at position (1, 1) on control pin 1 and D_j is placed at position (3, 4) on control pin 3. If droplet D_i moves to a new position (1, 2) from its initial position, the control pin 1 at the location (1, 1) is deactivated, and pin 2 at (1, 2) is activated accordingly. As a result, an unintentional splitting occurs for droplet D_j, since two direct neighbours of D_j with pin 2 are also getting activated.

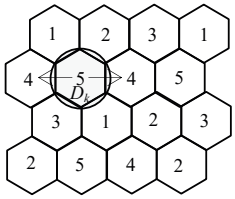

Fig. 5. Unwanted splitting of a droplet. Droplet D_k is split as pin 4 is activated that flanks pin 5 where D_k resides and which is deactivated.

Similarly, if there is another droplet D_k at position (2, 2) on pin 5 and we want to move it to position (2, 3), then the droplet may be confused about its destination. On pin location (2, 1) or (2, 3), as both of them are assigned the same control pin 4. So, inadvertent splitting occurs. This scenario is illustrated in Fig. 5. That type of unintentional movement, splitting, mixing of droplets may occur if proper pin assignment planning is not taken care of.

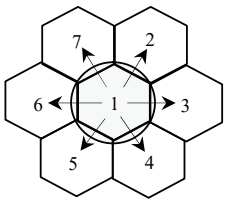

Fig. 6. A hexagonal cluster of size $N = 7$ and all possible movements of the droplet residing at control pin 1.

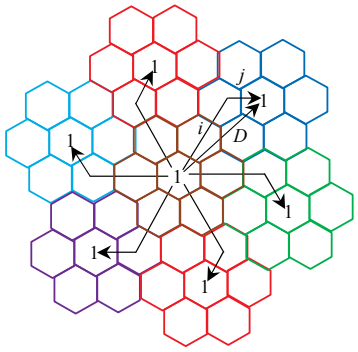

Fig. 7. Pin assignment in a 2D hexagonal array with shifting parameters $i = 2$ and $j = 1$ comprising seven clusters in a circular fashion. Control pin 1 is allocated to every cluster following the BSA-7 algorithm. Clusters centring a different pin are similar but different.

The problem of finding the minimum number of control pins to govern proper droplet routing without any interference on a 2D hexagonal electrode array is most likely to be a well-known graph colouring problem. As there are six sides of a hexagonal cell, we need a minimum of seven control pins to avoid unwanted mixing and splitting during droplet routing. The design process of pin allocation in each cell to overcome these constraints is termed as *pin reuse* or *pin planning*. Here seven cells comprising six around a central hexagonal cell construct a cluster of size $N = 7$ (see Fig. 6). Thus, the pin reuse factor in a cluster is 1/7.

Now, we are going to propose a new pin assignment algorithm in the 2D hexagonal electrode array, and this is termed as *Bridge Six Adjacent with 7 mutually different control pins* (BSA-7).

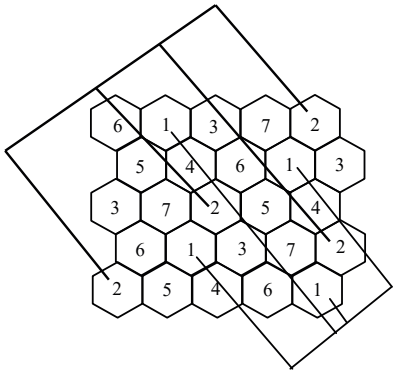

Fig. 8. Electrical wiring connection after the control pin assignment in HDMFB using BSA-7 algorithm.

Algorithm 1: BSA-7 algorithm

Input: A 2D regular hexagonal array.

Output: An assignment of control pins throughout the array so that no droplet interference occurs.

1: Assign an electrode (cell) on the 2D array with the numeric value '1', i.e. the control pin number of this cell.
2: Starting from this assigned cell, go straight to all directions through the sides and cover i number of cells.
3: Then take 60° clockwise turn and move j number of cells through the sides.
4: Assign the same pin number to the electrode (cell) reached.
5: Repeat steps 1 through 4 until all cells in the array are numbered. The adjacent cells must have different numbers.

In general, the above pin assignment problem belongs to the domain of NP-completeness that may be solved by using an approximation algorithm or a heuristic algorithm. The method of assigning control pin 1 using BSA-7 algorithm is shown in Fig. 7, where seven clusters are depicted, and the centre of the central cluster is labelled with pin 1.

Now starting from this cell, we can move along six possible directions. After traversing two cells in any direction, we take a 60° clockwise turn and move only one cell ahead. This cell is labelled as control pin 1. Here the cluster size becomes $N = 7$, while the shift parameters are $i = 2$ and $j = 1$. The closest distance between two cells (in two different clusters) using the same control pin (number) is termed as cluster distance or pin reuse distance, which is shown in Fig. 10. In HDMFB, four PCBs are required where

each PCB contains a pair of wiring connections. In Fig. 8, two wiring connections for pins 1 and 2 are shown in a single PCB layer.

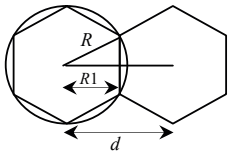

Fig. 9. Droplet on the charged hexagonal cell.

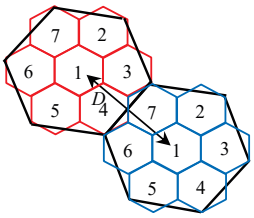

Fig. 10. Cluster distance or pin reuse distance (D), which is the same as the cluster diameter. Two clusters are shown with seven hexagonal electrodes in each with centring control pin 1.

D. The relationship between cluster size and shift parameters in a hexagonal electrode array

In Fig. 9, a droplet is placed on a charged regular hexagonal electrode with radius, R. Here $R1$ is the distance from the centre of the cell to its side. From this figure, we have $R1 = R\cos 30° = \sqrt{3}/2R$. Thus, the centre to centre distance between two adjacent hexagonal cells becomes $d = 2R1 = \sqrt{3}R$. Now, cluster distance, i.e. the center to center distance between any two adjacent clusters is D. As the center to center distance between two hexagonal cells is $\sqrt{3}R$, from Fig. 7, using the vector addition rule, it is clear that $D^2 = (\sqrt{3}Ri)^2 + (\sqrt{3}Rj)^2 - 2(\sqrt{3}Ri)(\sqrt{3}Rj)\cos 120° = 3R^2(i^2 + j^2 + ij)$.

It can be observed that the cluster distance is the same as pin reuse distance in any 2D hexagonal chip array. Also, pin reuse distance implies the centre to centre distance between two cells containing the same control pin. Thus, pin reuse distance is same as the cluster distance, D. The hexagonal cell area $A = 3\sqrt{3}/2R^2$ and cluster area $= \sqrt{3}/2D^2$. The cluster size N = cluster area / cell area $= (i^2 + j^2 + ij)$.

E. Routing constraints

The elemental step in any DMFB design is to formulate its fluidic constraints for safe droplet routing. The routing must ensure that the droplets reach to their intended destinations at different time stamps maintaining fluidic constraints. Two different droplets of the sample and/or reagent must not share the same electrode at the same time, and they must maintain a safe separation from each other.

The limitations for routing through HDMFB array are discussed here. While running an assay operation, no droplet should occupy the region of another droplet's cluster. This is shown in Fig. 11, where droplets D_i and D_j are placed at positions (4, 2) and (3, 3), respectively. Now D_j can move safely to its four adjacent cells, viz. (2, 3), (2, 4), (3, 4), and (4, 4). However, if D_j routes to the cell (3, 2) or (4, 3), then droplet interference occurs between D_i and D_j. Thus, D_j cannot move into the cluster region of droplet D_i. Again, as mixing operation is the most time-consuming part in any assay operation to get the desired result, the timing constraint states that the routing time in any assay operation should not exceed 10% of the total assay completion time.

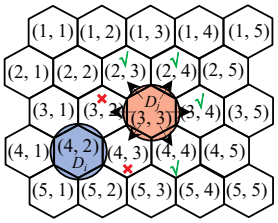

Fig. 11. Two droplets are placed on a 5×5 array. Droplet D_j's possible movements are shown by '√' and restricted movements are marked by '×'.

V. Experimental Results

Here, we mention some essential structural and behavioural features of HDMFB and compare it with the traditional square DMFB. To compare the scheduling span in terms of time based on colourimetric enzymatic reactions, we consider a multiplexed bioassay operation composed of glucose assay and lactate assay [1]. To perform the bioassay operations, we employ the concept of pin reuse while using the concept of time division pin sharing (TDPS) [1] as well as the routing constraints mentioned above. The sequencing graph of the operation above is shown in Fig. 12. The assay operation is simulated on a 15×15 2D square electrode array and a 15×15 2D regular hexagonal electrode array. The total elapsed times in both the scenarios are also estimated.

In a sequence graph, each vertex V represents an operation (i.e. dispensing of sample or reagent, mixing, detection, etc.) while an edge $e(i, j)$ denotes that the output of operation Oi is the input to operation Oj. Fig. 12 depicts a sequencing graph of an assay with eight operations, O1 through O8, where operations O1 through O4 are denoted as dispensing operations, I1 through I4, two mixing operations, O5 and O6 are shown as M1 and M2. Finally, two detection operations O7 and O8 represent D1 and D2, respectively.

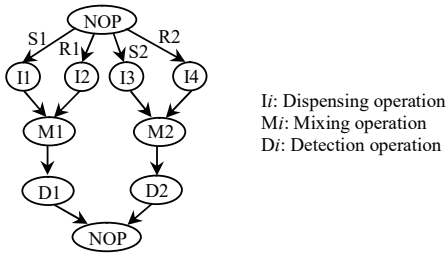

Fig. 12. Sequencing graph model for multiplexed bioassay. S1 and S2 are samples, R1 and R2 are reagents, M1 and M2 are mixing operations, D1 and D2 are detection operations, and NOP implies no operation.

The scheduling for bioassay execution is listed in Table I. Elapsed time is measured in unit time. The control pins after BSA-7 algorithm are assigned to the chip to perform the assay operations and to measure the total computation time. Sample reservoir, reagent reservoir, mixer module, and the detection zones are embedded on a 15×15 array, as shown in Fig. 14. Notably, the total assay completion time is the summation of mixing time and routing time (time taken

for the droplet for routing from source port (reservoir) to mixer module and then mixer module to detection port).

TABLE I

BIOASSAY SCHEDULING PLAN FOR A FULL ADDRESSABLE HDMFB.

Step	Time Elapsed (Unit)	Operation
Step 1	0.00 U	S1 and R1 initiate their routing towards the mixer zone.
Step 2	0.13 U	S1 and R1 reach to mixer zone.
Step 3	0.47 U	S1 and R1 are getting mixed.
Step 4	0.13 U	S2 and R2 reach to mixer zone.
Step 5	0.90 U	S1 and R1 start routing towards detection site and get detected.
Step 6	0.47 U	S2 and R2 are getting mixed.
Step 7	0.90 U	S2 and R2 start routing towards detection site and get detected.

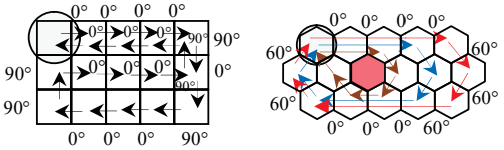

Fig. 13. (a) 3×5 mixer zone of square electrodes. (b) 3×5 mixer zone of hexagonal electrodes. The phase changes of the droplet trace are shown by arrows.

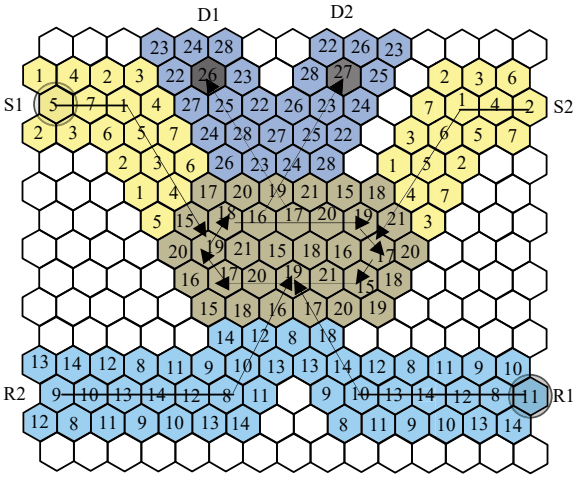

Fig. 14. A 15×15 array is used to accomplish a multiplexed assay operation. Here S, R, and D are the sample, reagent, and detection, respectively, and the mixer zone is a 3×5 hexagonal region. The droplet routing is shown by arrows.

Mixing is one of the decisive steps to realize a complete bioassay operation. The mixing action almost dominates performance analysis of the assay. In a microfluidic array the mixing operation can be performed anywhere and is not restricted to a specific portion on the chip, hence mixing can be termed as 'reconfigurable' operation [7], [9]. Inside a virtual module [10], mixing operations are executed by forming a group of adjacent electrodes as shown in Fig 14. Four types of movements may be assumed depending on the change of phases of a droplet route between two consecutive movements. They are forward movement (M_f), zigzag movement (M_z) [7], orthogonal movement (M_o), and backward movement (M_b) [9], [11] for the phase changes of 0°, 60°, 90°, and 180°, respectively. The active mixing is proportional to the rate of diffusion of the droplets [12], [13]. 0° movement yields the best outcome for mixing rather than 90° [7], [9]. 60° phase change is an intermediate stage between 0° and 90° [7].

Thus, it can be stated that $M_b < M_o < M_z < M_f$. According to the above claim since the movement towards 0° is most effective in terms of mixing, so in our mixer zone, we always keep two possible movements of the mixed droplet, such that 0° and 60°, and try to avoid the droplet movement with 120°. Applying such considerations, here we calculate the total mixing time required to complete the mixing operation in a 3×5 mixer of hexagonal cells (mixing cover up with 15 electrodes). Figure 13(b) shows the stated mixer module which is used in our assay operation.

TABLE II

LIST OF ACTIVATED PINS UNDER EXECUTION.

Step-wise performance	Activated control pin
Step 2	5, 7, 1, 5, 3, 4, 15 and 11, 8, 12, 14, 13, 10, 14, 18, 17
Step 4	2, 4, 1, 6, 5, 4, 21 and 9, 10, 13, 14, 12, 8, 10, 12, 16
Steps 3 and 6	18, 16, 17, 20, 19, 17, 15, 21, 19, 20, 17, 19, 18, 16, 17, 20, 16, 21, 19, 20, 21, 18, 16, 17, 18, 19, 20, 21, 18
Steps 5 and 7	19, 23, 28, 25, 26, 24 and 19, 24, 25, 23, 27, 26

Mixer module using 15 electrodes: Calculation of total mixing percentage (%age) and covering all electrodes

Percentage (%age) of mixing due to four consecutive phase changes of 0° + %age of mixing due to three consecutive phase changes of 60° + %age of mixing due to three consecutive phase changes of 0° + %age of mixing due to three consecutive phase changes of 60° + %age of mixing due to two consecutive phase changes of 0° + %age of mixing due to three consecutive phase changes of 60° + %age of mixing due to two consecutive phase changes of 0° + %age of mixing due to three consecutive phase changes of 60° + %age of mixing due to one 0° phase change + %age of mixing due to five consecutive phase changes of 60° + %age of mixing due to two consecutive phase changes of 0° = 2.9 + 0.8 + 1.74 + 0.8 + 0.87 + 0.8 + 0.87 + 0.8 + 0.29 + 1.8 + 0.87 = 12.54.

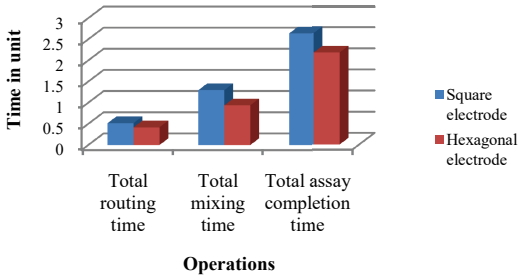

Fig. 15. Performance of square array and HDMFB.

We implement our proposed algorithm in JAVA on a computer with a 2.40 GHz Intel Core *i*5 CPU and 4 GB RAM, running a 64-bit Windows operating system. Fig. 15 exhibits the routing performance, mixing time, and total assay completion time of square electrode array and hexagonal electrode based array. From the figure, it is evident that the effectiveness of this closed packing HDMFB is better than the conventional square electrode array.

A comparative study between square and hexagonal chip array has been depicted in Table III. Total time required to complete the whole mixing operation is 0.47 sec [7], [10]. However, the time necessary in case of 3×5 square mixer array for the same assay operation is 0.65 sec [9]. As a good mixing procedure provides a better and accurate result, any mixing operation should take much more attention and time compared to that of routing operation. In the case of hexagonal electrodes, the types of droplet movement could be five as well, if we allow 120° phase change, if necessary, beyond the aforementioned phase changes of 0°, 60°, 90°, and 180°.

TABLE III

COMPARISON BETWEEN SQUARE AND HEXAGONAL ELECTRODE ARRAY.

Type of electrode	Square electrode	Hexagonal electrode
Length of one side	a	0.58a
Overlapping length	0.207a	0.207a
The gap between two consecutive electrodes	a/2	a/2
Number of direct neighbours	Four	Six
Area of electrode	a^2	0.87a^2
Minimum pin requirement	Five	Seven
Number of PCB required	Three	Four
Mixer Zone	Rectangular	Hexagonal
Mixing time	0.65 sec for 3×5 mixer	0.47 sec for 3×5 mixer
Droplet trace	Straight	Straight and Zigzag
Droplet movement	Along four directions	Along six directions
Types of movement of the droplet	Three; 0°, 90°, and 180°	Four; 0°, 60°, 90°, and 180°

The whole array is subdivided into four partitions following the time division pin sharing (TDPS) concept. According to our operational steps which are mentioned in Table I, the control pins are fabricated on the array using the BSA-7 algorithm. Then to perform the bioassay operations without any interference the concept of TDPS is applied to it. Using the notion of TDPS, Table II is created. Fig. 14 represents the multiplexed bioassay with proper routing paths, mixer module, and the appropriate control pins which are taken into consideration.

VI. CONCLUSION

In this paper, we propose a new design technique of DMFB which is supposed to be a better alternative over the array of square electrodes. Again, as mixing is the most critical operation in case of any diagnosis procedure, this architecture performs better. In the case of conventional hexagonal electrodes, the droplet can traverse along six different directions, and its speed is also high enough. Here the droplet can move in the direction of 60° angle (in a zigzag motion) and even in the forward direction; thus, the mixing procedure is undoubtedly better than that in a square electrode array (within a specified time period).

Every design technique has its benefits and discrepancies, which is equally true for our designed architecture and method as well. Since a droplet can move in six possible directions on a regular hexagonal electrode array, so the routing time is also reduced than that required in the case of the conventional square electrode array. In the hexagonal electrode array, the total number of control pins is marginally increased. As the mixing operation dominates the routing time, it is considered to be a successful shift to a new design concept.

REFERENCES

[1] F. Su, K. Chakrabarty, and R. B. Fair, "Microfluidics-Based Biochips: Technology Issues, Implementation Platforms and Design- Automation Challenges", IEEE Transactions on Computer Aided Design of Integrated Circuits and Systems, vol. 25, no. 2, 2006, pp.211-223.

[2] K. Chakrabarty and T. Xu, "Digital Microfluidic Biochips: Design Automation and Optimization", CRC Press, USA, 2010.

[3] K. Chakrabarty and F. Su, "Digital Microfluidic Biochips, Synthesis, Testing and Reconfiguration Techniques", CRC Press, USA, 2007.

[4] R. B. Fair, "Digital Microfluidics: Is a True Lab-on-a-Chip Possible?" Microfluid Nanofluid, Springer, vol. 3, 2007, pp. 245-281.

[5] K. Chakrabarty, R. B. Fair, and J. Zeng, "Design Tools for Digital Microfluidic Biochips: Towards Functional Diversification and More than Moore", IEEE Transactions on Computer-Aided Design of Integrated Circuits and Systems, vol. 29, no. 7, 2010, pp. 1001-1017.

[6] L. Schneider, O. Keszocze, J. Stoppe, and R. Drechsler, "Effects on Cell Shapes on the Routability of Digital Microfluidic Biochips", Design, Automation and Test in Europe (DATE) conference, 2017, pp. 1631-1634.

[7] P. Datta, A. Dutta, R. Majumder, A. Chakraborty, D. Dhal, and R. K. Pal, "A Design of Digital Microfluidic Biochip along with Structural and Behavioural Features in Triangular Electrode Based Array", Procedia Computer Science, vol. 93, 2016, pp. 183-190.

[8] F. Su, K. Chakrabarty, and V. K. Pamula, "Yield Enhancement of Digital Microfluidics-Based Biochips using Space Redundancy and Local Reconfiguration", Design, Automation and Test in Europe (DATE) conference, 2005, pp. 1196-1201.

[9] P. Paik, V. K. Pamula, and R. B. Fair, "Rapid Droplet Mixers for Digital Microfluidic Systems", The Royal Society of Chemistry, 2003.

[10] E. Maftei, P. Pop, and J. Madsen, "Droplet-Aware Module-Based Synthesis for Fault-Tolerant Digital Microfluidic Biochips", DTIP 2012 / ©EDAPublishing, 2012.

[11] P. Paik, V. K. Pamula, and R. B. Fair, "Rapid Droplet Mixers for Digital Microfluidic Systems", Lab-on-a-Chip, 2003, pp. 253-259.

[12] K. Chakrabarty, "Design Automation and Test Solutions for Digital Microfluidic Biochips," IEEE Transactions on Circuits and Systems, vol. 57, no. 1, 2010, pp. 4-17.

[13] H. C. Chang and L. Yeo, "Electrokinetically Driven Microfluidics and Nanofluidics", New York, Cambridge University Press, 2009.